Soldagem & Inspeção

Influence of Push and Pull Techniques on High-Speed Buried-Arc GMAW Process

Natália Wendt Dreveck[1,2], Luiz Delagnelo Barbetta[2], Danielle Bond[1] (iD), Guilherme Ourique Verran[1]

[1] Universidade do Estado de Santa Catarina – UDESC, Centro de Ciências Tecnológicas, Joinville, SC, Brasil.
[2] Instituto Senai de Inovação em Sistemas de Manufatura e Processamento a Laser, Joinville, SC, Brasil.

Abstract: The GMAW torch orientation, whether pulling or pushing, influences both arc welding and hybrid processes. In hybrid laser-arc welding, for example, when the torch is pulled, a greater bead penetration is obtained. To promote greater penetration, the literature also indicates the use of a buried arc in GMAW, although it was initially developed to only operate with a vertically-positioned torch. Therefore, this work aims to investigate the influence of the push and pull techniques on the behavior of buried-arc GMAW at high welding speeds. Welds were performed with the push and pull techniques under the following conditions: buried and unburied (long) arc with welding speeds of 1.0, 1.5 and 2.0 m/min and current ranging from 450 to 470 A. The process tends to be more stable when pulling than when pushing (buried or long arc). Evidence of instability was only identified for the pushed buried arc, due to material accumulation at the front region of the molten pool, for the higher welding speeds. Only the 1.0 m/min buried-arc processes resulted in beads with an appropriate surface finish.

Key-words: Buried arc; GMAW stability; Molten pool; Humping.

1. Introduction

When joining thick structural steel plates, welding processes such as Gas Metal Arc Welding (GMAW) and Submerged Arc Welding (SAW) are generally used. In those applications, several passes and a large amount of deposited material are required to fill the groove. Despite the consolidated use of such processes by the industry, the search for increased productivity and cost reduction leads to the need for new procedures and for the improvement of existing technologies. One way to increase productivity in those operations is by increasing the welding current and speed [1], and the buried-arc GMAW is a process that allows such changes.

In this process, a high current combined with a forcibly short arc creates a depression in the molten pool, which allows the arc to establish and operate in a region below the base metal surface [2,3]. This GMAW version has high deposition rates due to the high wire-feed speeds required to keep the short arc length and to the high currents combined with the long stick-out, which assist in wire fusion. According to Dompablo [2], the buried arc yields a highly productive, high-penetration and undercut-free process. Furthermore, the potential speed increase results in smaller heat affected zones and distortions when compared to the conventional process. Schroepfer et al. [4] also pointed out that this process allows the welding of narrower joints with narrower groove angles.

Another process employed when welding high-thickness plates is the hybrid laser-arc welding (HLAW). The laser is responsible for ensuring penetration while the GMAW makes the process more robust, providing the appropriate amount of filler metal, while enabling the addition of alloy elements to the application [5]. Two configurations can be used in the application of HLAW: arc leading or laser leading, resulting in the pull (arc leading and laser vertically behind) and push (laser leading vertically and tilted arc behind) configurations for the GMAW process. The arc leading case presents greater penetration, considering that the laser falls onto the molten pool surface, where absorption is greater [6]. That is a desirable condition when working with thicker plates and results in highly reinforced narrow beads, albeit there is greater undercut tendency [7]. The laser leading condition tends to be more stable [6] and the resulting bead is wider and shallower than in the process with the arc leading.

One of the difficulties of working with hybrid laser-arc welding is the high cost of laser equipment, especially for high power levels. To lower costs using lower-power lasers, while still ensuring high penetration and/or welding speed, the buried arc operation can be adopted, as described by Gook et al. [8], Pan et al. [9] and Wahba et al. [10]. Those works used laser pulled buried-arc GMAW, and this process was originally developed for vertical torch operation [11]. Most of the published works on buried-arc GMAW still use the torch in such position [3,4,12,13]. Therefore, the literature lacks works approaching the push and pull techniques in the buried-arc GMAW. In addition, few studies have evaluated the buried arc at high speeds, above 1 m/min, which are usually

applied in hybrid processes. The buried arc application has been studied at speeds between 0.35 and 0.60 m/min [3,12,14,15], 0.8 and 1.4 m/min [16] and 0.7 and 1.8 m/min [13].

Therefore, aiming at a later application in the hybrid GMAW-laser welding process, this work aims to investigate the influence of the push and pull techniques on the behavior of the buried-arc GMAW at high welding speeds.

2. Materials and Methods

To evaluate the behavior of the push and pull techniques with buried-arc GMAW, welds were performed with both techniques under the following conditions: buried and unburied arc (called "long arc" in this work) with welding speeds (S) of 1.0, 1.5 and 2.0 m/min, and current ranging from 450 to 470 A.

The welds in this work were carried out, in the flat position, with simple deposition on ABNT 1020 carbon steel plates (300 mm wide, 400 mm long and 12 mm thick), with AWS ER70S-6 type wire filler metal (1.2 mm diameter), argon + 18% CO_2 shielding gas with a 20 L/min flow rate, contact tip to work distance (CTWD) fixed at 15 mm and torch tilt angle of 50°.

A Digiplus A7 PMDAC-1000 multiprocess welding source was used in constant-voltage mode and the parameters were set so that the average current would stay between 450 and 470 A at a welding speed of 1.0 m/min and replicated for the other speeds. A high wire-feed speed and a lower voltage were used for the buried-arc process, forcing a reduced arc length [2]. Table 1 shows that a small voltage increase in the push mode was necessary to reach the desired current, with both the buried and the long arcs. Each condition was then repeated twice.

Voltage and current data were collected during all tests using a data acquisition system (SAP V4) from the welding source itself. The mean voltage (Vm) and mean current (Im) in Table 1, were calculated by the SAP V4 software and refers to one of the weld replicas. Later, the data was analyzed through software to compare the stability of the welding conditions using voltage and current oscillograms and cyclograms.

Table 1. Welding process parameters.

Technique	Arc	Set Parameters			Measured Parameters	
		S (m/min)	V (V)	F (m/min)	Vm (V)	Im (A)
Pull	Buried	1.0	35	18	36	456
	Buried	1.5	35	18	36	470
	Buried	2.0	35	18	36	464
	Long	1.0	40	14	41	466
	Long	1.5	40	14	41	459
	Long	2.0	40	14	41	462
Push	Buried	1.0	37	18	38	461
	Buried	1.5	37	18	40	461
	Buried	2.0	37	18	38	462
	Long	1.0	42	14	43	464
	Long	1.5	42	14	43	470
	Long	2.0	42	14	43	456

Observation: S: welding speed; V: voltage; F: wire-feed speed; Vm: mean voltage; Im: mean current.

To view the arc and measure its length, a high-speed camera with a 320 × 240 pixels resolution, a 20000 frames-per-second image-acquisition rate, a 5 μs exposure time and an f/16.0 lens aperture was used. No filters were used when filming the electric arc. The image was adjusted using settings in the high-speed camera software, PCC 3.1 (Phantom Camera Control Application). To evaluate the metal transfer, a Cavitar Cavilux Smart illumination laser and a filter for the laser wavelength range were used. Figure 1 shows the reference used to measure the arc length and a side-view schematic representation of the torch set-up, while Figure 2 shows the front view of the experimental arrangement used in the tests. The high-speed camera was placed at the side of the table, so that the torch tilt could be observed. During the welding operations, a system that allows the use of a static torch with the movement of the base material was used.
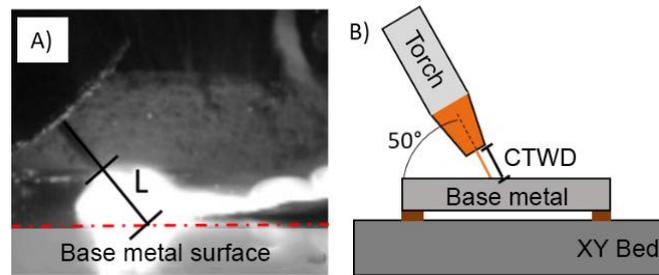
Figure 1. (A) reference used to measure the arc length (L); and (B) side view of the torch set-up.
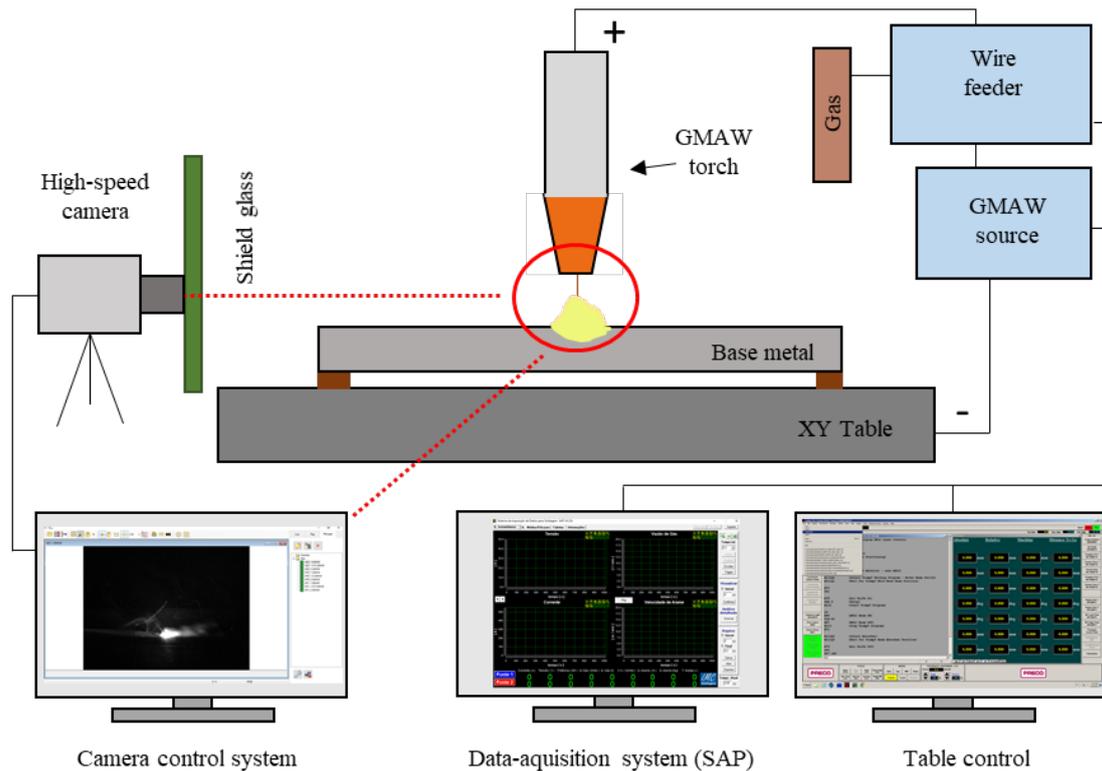

Figure 2. Schematic representation of the experimental arrangement used in the tests (perpendicular to the welding direction).

3. Results and Discussion

It is important to start by saying that the definition of a buried-arc process differs in the literature. Some authors use the buried arc as a metal-transfer designation [17] while others see it as a process characteristic [3]. Using the buried arc to characterize the process seems more appropriate since, during its use, different metal transfers can be observed [3], like projected-spray, streaming-spray and rotating-spray transfers. Stol et al. [13] even use the acronym GMBAW (Gas Metal Buried Arc Welding) to refer to the process.

Despite the differences, it is agreed that the arc must be in a region close to or below the base metal surface, within a depression in the molten pool [4,10], which is possible due to the high pressure resulting from the used current, combined with a high wire-feed speed and a low voltage. Such parameter combination results in a forcibly short arc that is established in a depression within the pool of molten material. This behavior was observed during welding operations throughout this work, as shown in Figure 3. Therefore, the chosen parameters, under the conditions evaluated in this study, resulted in buried-arc GMAW. The shape of the molten pool in the buried-arc process could also be observed. It shows the same behavior as what the literature indicates with the use of an unburied arc. The molten pool produced by the pull method is narrow and elongated, the opposite of what is observed from the push technique. The different morphology between them is explained by the characteristics of the arc's incidence surface. When the push orientation is used, the arc is directed at the solid portion of the base metal, which tends to laterally spread the molten metal, while when the pull technique process is used, the arc is directed at the molten pool, favoring penetration and the elongation of the pool [18]. At higher welding speeds, the molten pool length-width ratio is higher, as the pool becomes more elongated, and the heat input decreases [19]. Therefore, the depression observed inside it is expected to be narrower and shallower at 2.0 m/min than is was observed at 1.5 m/min, and larger and deeper at 1.0 m/min.
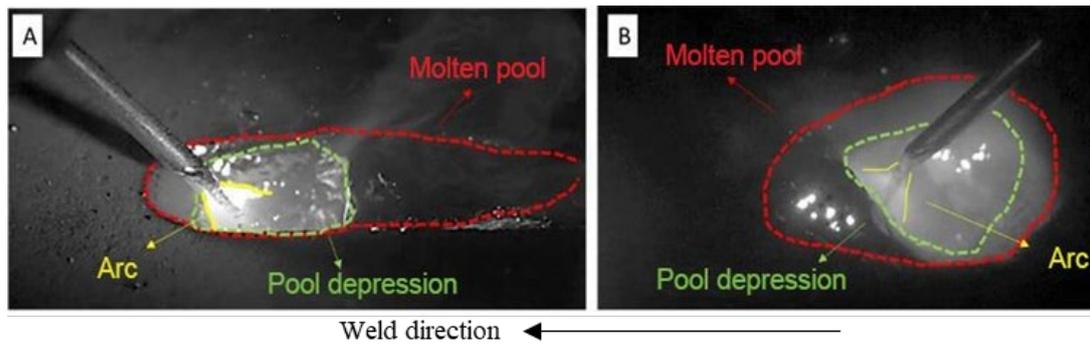
Figure 3. Molten pool characteristic in pulled (A) and pushed (B) buried-arc GMAW techniques, with a welding speed of 1.5 m/min.

The images of the electric arc captured during welding under the conditions determined according to Table 1 are shown in Figure 4. The images show that, under the buried-arc condition, the arc is shorter (1.0 to 1.7 mm) when compared to the long arc (5.1 to 5.6 mm), as expected; as well as the pull technique (1.0 to 1.6 mm), which used 36 V, if compared to the push technique (1.2 to 1.7 mm), which used 38 to 40 V. The lower values when pulling were expected since the arc length is proportional to the voltage [20].
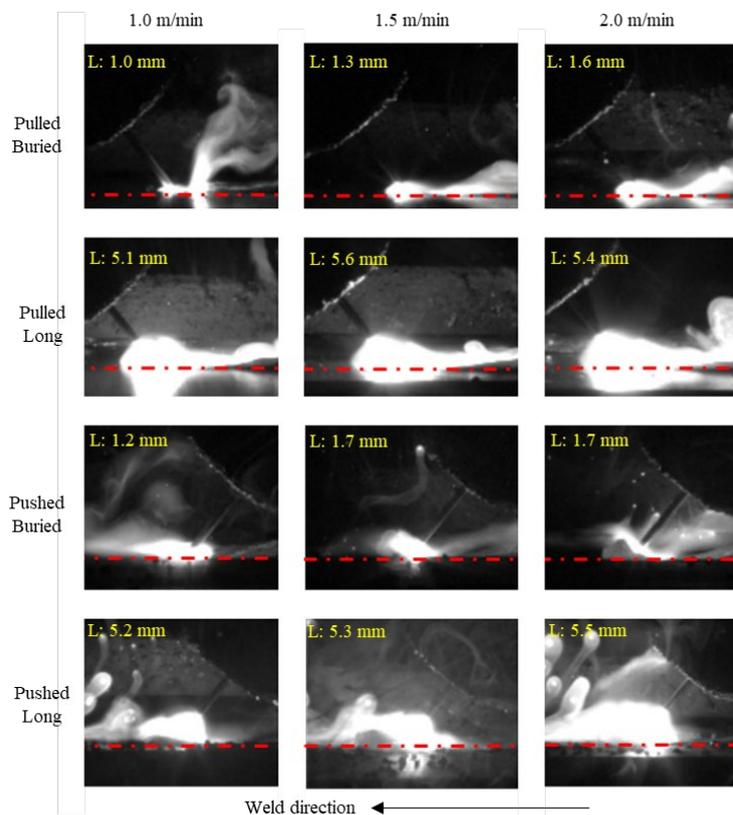

Figure 4. High-speed camera images for each studied condition, showing the difference in arc length (L).

To assess the stability of the welding processes, the current and voltage can be presented through cyclograms. According to Suban and Tusek [21], cyclograms are a practical and simple interpretation tool to evaluate process stability and repeatability. This same technique has already been used to assess the stability of the FCAW process [22] and with a coated electrode [23], showing that, despite being commonly applied to the GMAW process with short-circuit transfer, cyclograms can also be used in complementary assessments for the other processes and metal transfers. The more concentrated and closer to overlapping the lines of the same cycle region, the more stable the process, while the presence of dispersed lines shows an unstable operating condition [21, 22, 24].

In this work, the high-speed camera images taken of the buried-arc GMAW, in the pull and push positions, with a 1.5 m/min welding speed, confirm the occurrence of the spray transfer, as shown in Figure 5. The metal transfer was not recorded for the

processes with 1.0 and 2.0 m/min welding speeds, but they supposedly also exhibited a metal transfer in the spray range. This supposition is backed by the oscillograms, Figure 6, and the cyclograms, Figure 7, obtained under the studied welding conditions, which have characteristics corresponding to the spray metal transfer. In the oscillograms, the current is in a constant range over time [25]; in the cyclograms, the current and voltage signals are concentrated in a certain region [21]. The spray metal transfer was expected, since the transition current for the ER 70S-6 wire with 1.2 mm diameter, using 15 mm CTWD and an argon-based shielding gas with 15% CO_2, is in the range between 210 and 230 A [26], lower than the currents applied in this study (ranging from 450 to 470 A). Although Figure 5 shows a molten and elongated end of the filler metal, which, according to the IIW classification, is characteristic of the streaming-spray transfer, which free-flight transfer occurred for each welding speed is not exactly certain. Wahba et al (2015) observed both streaming and projected spray in the same weld bead [27] and this phenomenon could also happen in all the processes and welding speeds studied in this paper.
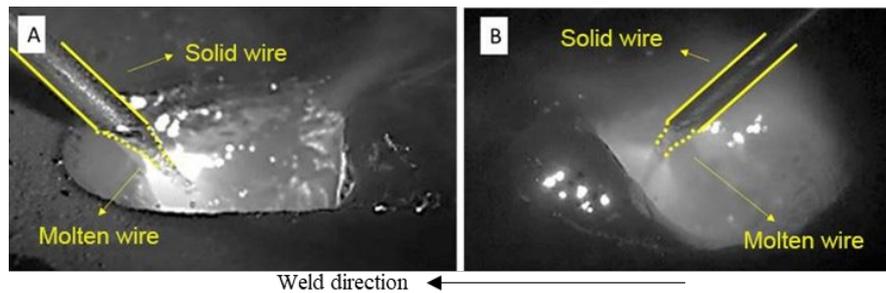

Figure 5. Metal transfer observed in pulled (A) and pushed (B) buried-arc GMAW techniques, with a welding speed of 1.5 m/min.

Figure 7 shows that the current and voltage signals are concentrated in a single region of the graphs. Considering that the more concentrated the signals, the more stable the process [21], both pull-configuration techniques (buried and long arc) presented more stable characteristics than the push ones.

The pushed buried-arc welding presents greater instability when compared with the long arc, and it gets even worse as the speed increases (Figure 7G, 7H, 7I). Initially, this could be related to the reduction of the thermal input, which occurs at higher speeds, resulting in a smaller amount of molten material and a smaller molten pool [18]. The reduced molten pool volume can yield a narrower depression, which could increase instability.

Another way of assessing the occurrence of spray transfer and process stability is a feature of the data acquisition system software, SAP V4, which analyzes the number and duration of short circuits that may occur during the welding process. Ideally, short circuits should not occur during spray transfer, therefore, the number of short circuits detected by the software and their average duration should be zero [25]. Table 2 brings such analysis using data regarding the welding processes (same data range used in the cyclograms). Short circuits were identified only in the pushed buried-arc cases, corroborating the unstable aspect observed under that condition in both oscillograms and cyclograms.
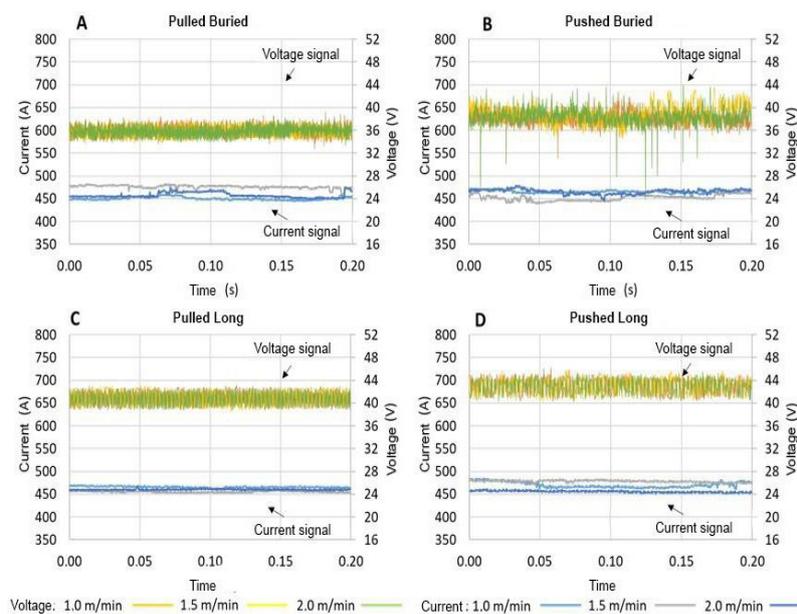

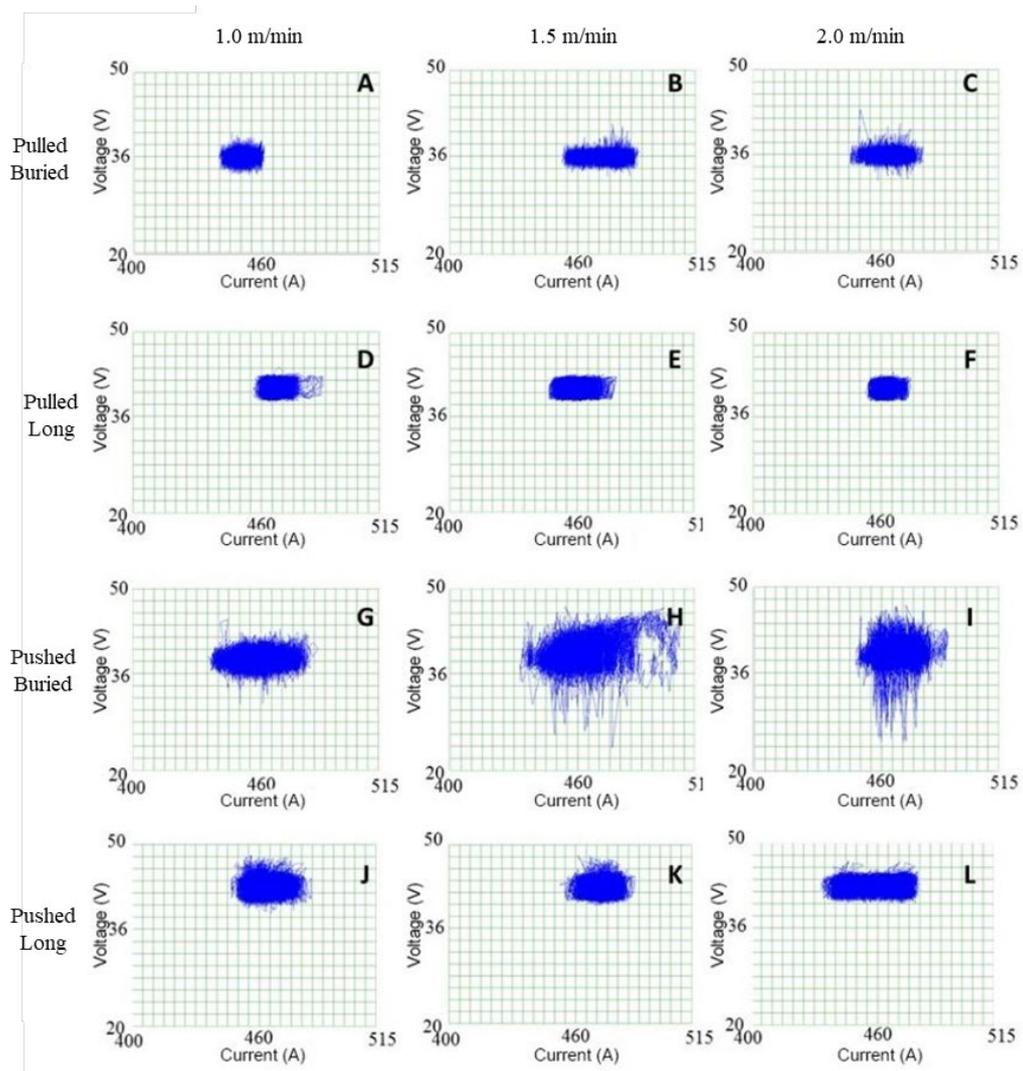**Figure 6.** Oscillograms for the welding conditions (A-D) studied.

Figure 7. Current and voltage cyclograms for all conditions (A-L) studied.

Table 2. Number and duration of short circuits identified during the processes.

Process	S (m/min)	Number of identified short circuits	Average duration of short circuits (ms)
Pulled Buried	1.0	0	0.0
	1.5	0	0.0
	2.0	0	0.0
Pulled Long	1.0	0	0.0
	1.5	0	0.0
	2.0	0	0.0
Pushed Buried	1.0	5	0.2
	1.5	139	0.2
	2.0	179	0.2
Pushed Long	1.0	0	0.0
	1.5	0	0.0
	2.0	0	0.0

The resulting images from the long-arc welding processes turned out differently for the push and pull techniques. Image acquisition and treatment was the same for all cases, so the grayish aspect of the pushed long-arc process (Figure 8) results from the presence of a great presence of fumes. Those conditions yielded more spatters than the other processes. Through the

analysis of the high-speed footage, the spatters is observed to originate from a region close to the front end of the molten pool. The spattering is supposedly droplets of molten metal that splash out of the molten pool due to the pressure from the plasma jet, and are not caused by instabilities in the voltaic arc and/or metal transfer, once the oscillograms (Figure 6) and the cyclograms (Figure 7) show a stable process with no short circuiting under these conditions.
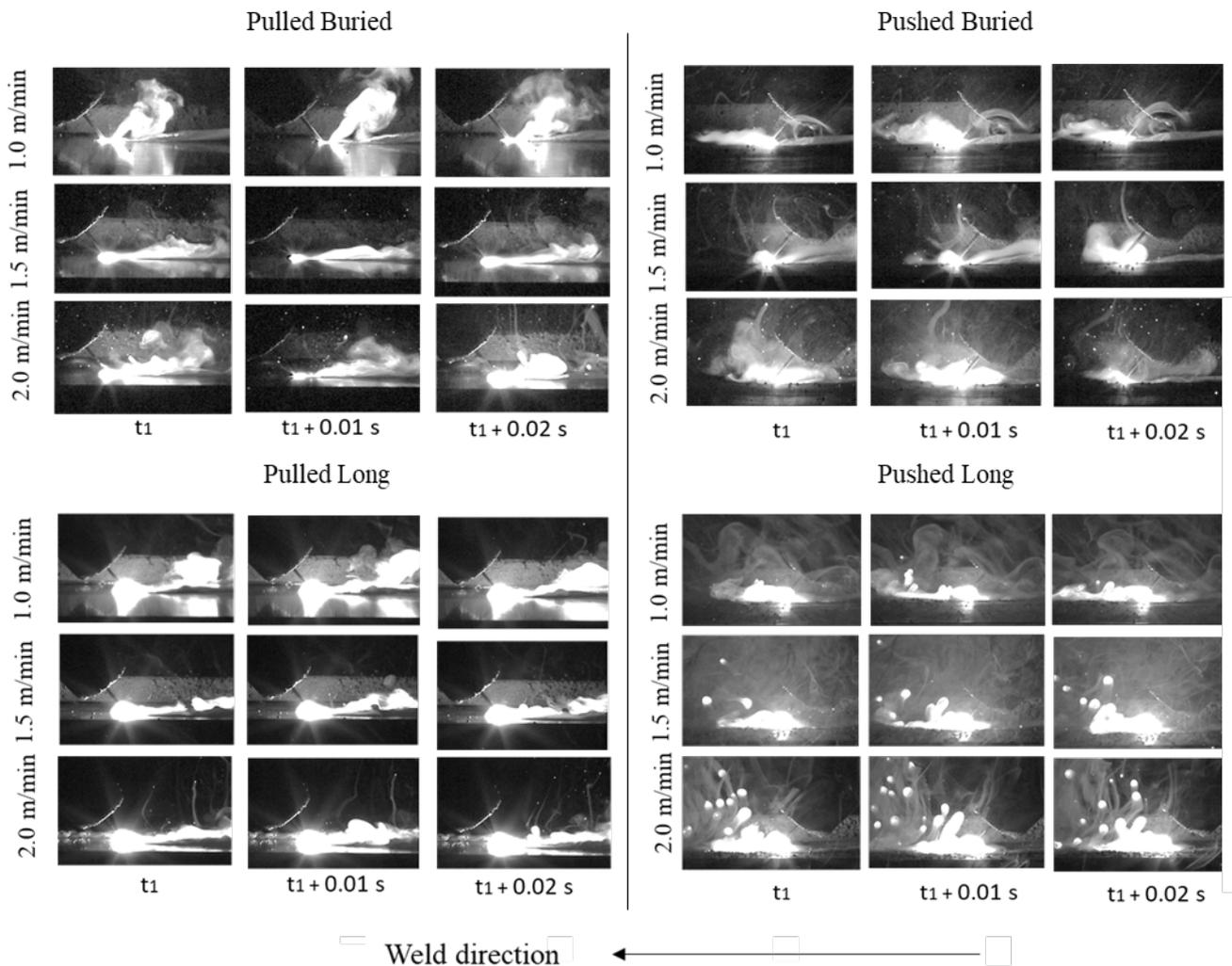

Figure 8. High-speed camera images for different moments of the processes, starting from instant "t1".

In buried-arc processes, the presence of fumes and spatters was small and the same behavior was shown by Pan et al. [9]. During the pulled buried-arc technique, disturbances are observed in the high-speed camera images as brief moments when the arc luminosity gets dimmer. In the pushed buried-arc technique, the instabilities occurred when the wire touched an molten material build up in the front region of the molten pool. Such material accumulation can be observed throughout the process with welding speeds of 1.5 and 2.0 m/min, while no inconsistency is observed at 1.0 m/min (Figure 9). A moment of the process (at 2.0 m/min) where instability occurs due to the interaction of the arc with the material accumulation (Figure 10) is highlighted. At time t, the arc can be observed near the accumulated material. At t + 0.001 seconds, the arc brightness region is reduced due to the proximity between the wire tip and the accumulated material. At t + 0.002 seconds, the region and arc brightness suddenly increase, a similar behavior to what is observed at the voltaic arc re-ignition moment after a short circuit.
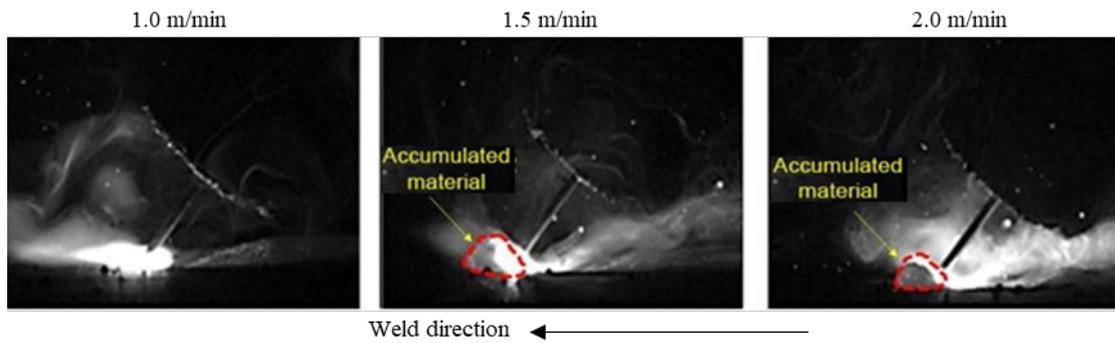
Figure 9. Accumulated material at the front end of the molten pool, observed in the pushed buried-arc technique.
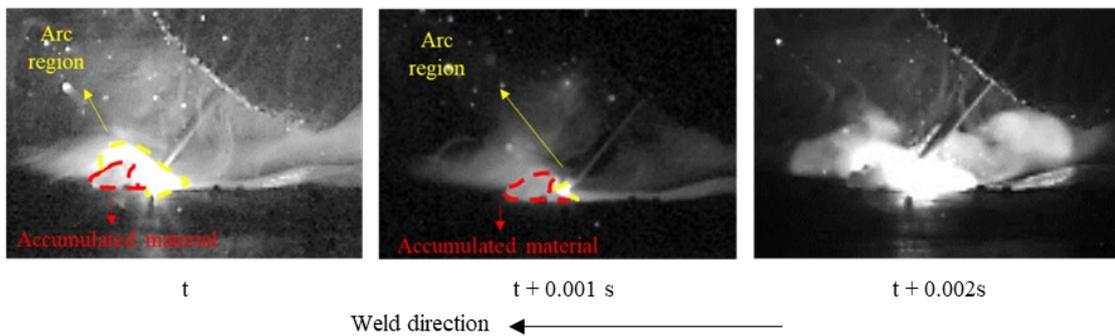

Figure 10. Instability observed in the pushed buried-arc technique, 2.0 m/min, starting from instant "t".

The accumulated material can also be observed in the high-speed camera images acquired to verify the metal transfer and molten pool depression (Figure 11A). The high pressure applied by the buried-arc plasma jet supposedly pushes the molten material against the solid surface at the front interface between the base metal and the molten pool, causing part of the flow to be directed upwards (schematics in Figure 11B).
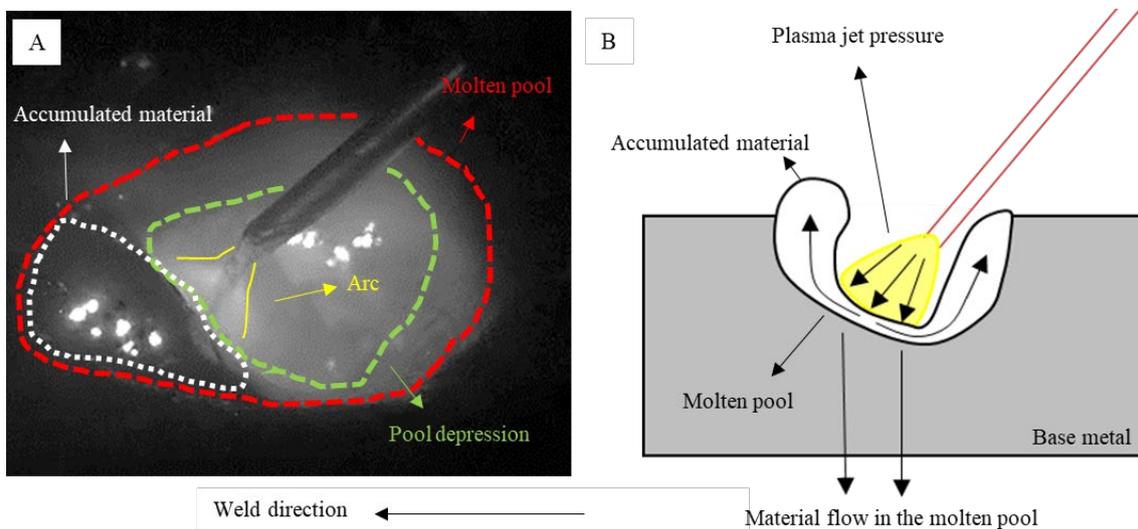

Figure 11. (A) Accumulated material in the front region of the molten pool in the pushed buried-arc technique and 1.5 m/min welding speed; (B) Representation of material accumulation formation.

Figure 12 shows the beads produced according to the studied parameters. High-speed and high-current welding is often limited by the presence of discontinuities such as humping and undercuts [1], as well as in the beads produced at higher speeds (1.5 and 2.0 m/min). Unlike the laser welding process, which can use high welding speeds, even above 5 m/min [28]. For 1.0 m/min, both buried-arc conditions yielded better beads than those obtained with an equivalent long arc, indicating that the buried arc can be a solution to extend the process window for higher speed and current conditions. Even the beads showing

stable characteristics in the oscillograms and cyclograms have defects and irregularities. Such behavior shows that, in the welding process analysis, more than one evaluation methodology must be considered in order to properly characterize the process.

It is interesting to observe that the types of discontinuities and their evolution were different between the welding conditions. The pulled buried-arc technique resulted, for speeds of 1.5 m/min or faster, in beaded cylinder morphology (BCM) humping, according to the classification of Soderstrom and Mendez [29], usually associated with long and narrow molten pools [30,31], which are obtained when high welding speeds are employed. The long arc, in turn, with the same technique, is marked by discontinuities associated with instabilities in the pool's gouging region such as: gouging region morphology humping (GRM), tunnel porosity and formation of three-part split beads, two at the edges and one at the center. Tunnel porosity and GRM humping dominate the bead for a 1.0 m/min speed, while the split beads, with each division still affected by BCM humping, predominate at higher speeds.
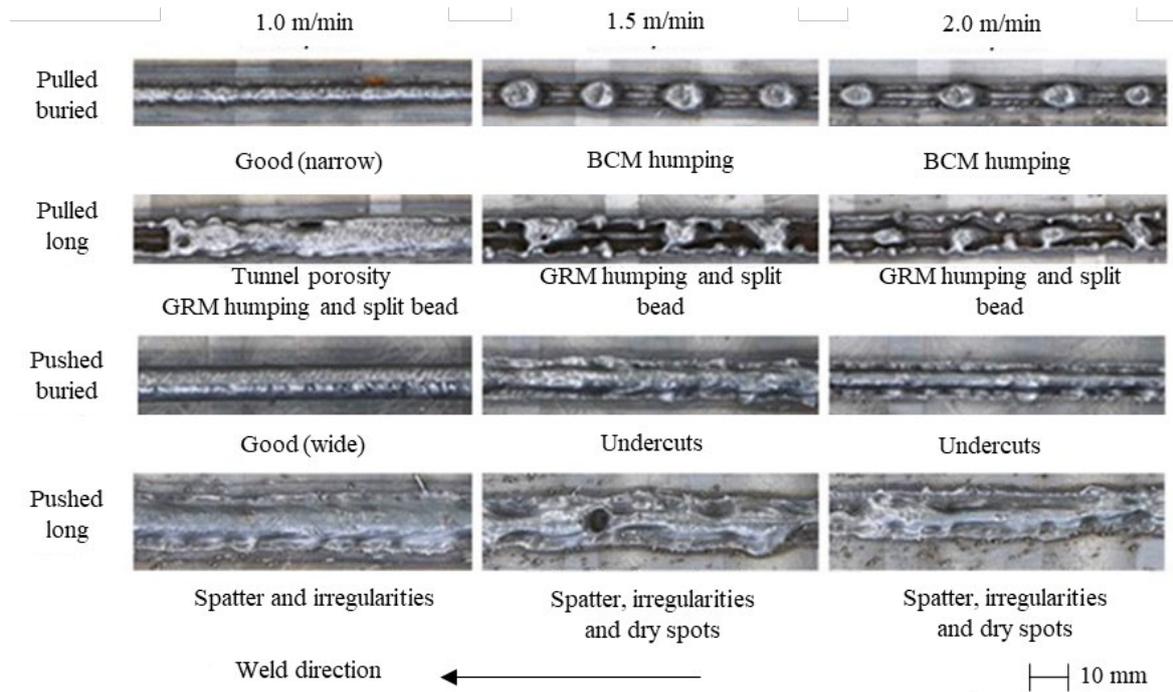

Figure 12. Weld beads resulting from each process.

With a pushing torch, the buried arc yielded humping-free beads, albeit with the presence of undercuts for speeds over 1.5 m/min. Such undercuts might be caused by the premature solidification of the bead edges in the gouging region [1,31,32]. The long arc, on the other hand, yielded irregular beads, with increasing irregularities proportional to the welding speed, and with the formation of sparse dry spots starting from 1.5 m/min. Dry spots are, normally, linked to premature solidification of the gouging region, which can also lead to the formation of GRM humping [1,31,32]. Thus, those welds are possibly on the verge of starting the GRM humping, which could explain the bead irregularity.

4. Conclusions

This work shows that the push and pull techniques interfere in the buried-arc GMAW stability, which can guide the optimization of a future hybrid laser-arc welding process. In the buried-arc GMAW process, the arc is established in a depression in the center of the molten pool, which is narrow and long for the pulling technique, and wide and short for the pushing one. The metal transfer observed within the depression, for the studied parameters, was the streaming spray.

The obtained cyclograms show that, in general, the pulling technique tends to be more stable than the pushing one, for both the buried and the long arc. Besides, signs of process instability, in the form of short circuits, were only identified for the pushed buried-arc technique. This condition's greater instability seems to result from an accumulation of material at the front region of the molten pool, for the highest studied welding speeds. Only the pushed and pulled buried-arc techniques with a welding speed of 1.0 m/min resulted in beads with an appropriate surface finish. For all other processes, the high welding speeds yielded beads with a high incidence of humping and undercuts.

Therefore, the pull technique in the buried-arc GMAW seems to be a better option for hybridization with laser beam (tilted arc leading and laser vertically following behind).

References

[1] Mendez PF, Eagar TW. Penetration and defect formation in high-current arc welding. Welding Journal. 2003;82(10):296.

[2] Dompablo M. New solutions in coldArc and forceArc welding technology. Welding International. 2013;27(1):24-29. http://dx.doi.org/10.1080/09507116.2011.600020.

[3] Baba H, Era T, Ueyama T, Tanaka M. Single pass full penetration joining for heavy plate steel using high current GMA process. Welding in the World. 2017;61(5):963-969. http://dx.doi.org/10.1007/s40194-017-0464-7.

[4] Schroepfer D, Kromm A, Kannengiesser T. Optimization of welding loads with narrow groove and application of modified spray arc process. Welding in the World. 2017;61(6):1077-1087. http://dx.doi.org/10.1007/s40194-017-0484-3.

[5] Olsen FO. Hybrid laser-arc welding. 1st ed. Cambridge: Woodhead; 2009. 323 p. http://dx.doi.org/10.1533/9781845696528.

[6] Zhiyong L, Srivatsan TS, Yan LI, Wenzhao Z. Coupling of laser with plasma arc to facilitate hybrid welding of metallic materials: a review. Journal of Materials Engineering and Performance. 2013;22(2):384-395. http://dx.doi.org/10.1007/s11665-012-0280-6.

[7] Bunaziv I, Akselsen OM, Ren X, Salminen A. Hybrid welding possibilities of thick sections for arctic applications. Physics Procedia. 2015;78:74-83. http://dx.doi.org/10.1016/j.phpro.2015.11.019.

[8] Gook S, Gumenyuk A, Rethmeier M. Hybrid laser arc welding of X80 and X120 steel grade. Science and Technology of Welding and Joining. 2014;19(1):15-24. http://dx.doi.org/10.1179/1362171813Y.0000000154.

[9] Pan Q, Mizutani M, Kawahito Y, Katayama S. Effect of shielding gas on laser-MAG arc hybrid welding results of thick high-tensile-strength steel plates. Welding in the World. 2016;60(4):653-664. http://dx.doi.org/10.1007/s40194-016-0333-9.

[10] Wahba M, Mizutani M, Katayama S. Microstructure and mechanical properties of hybrid welded joints with laser and CO_2 shielded arc. Journal of Materials Engineering and Performance. 2016;25(7):2889-2894. http://dx.doi.org/10.1007/s11665-016-2137-x.

[11] Stol I, Williams L. Gas metal buried arc welding of LAP - penetration joints. United States patent US 6828526. 2004 Dec 7.

[12] Heinze C, Michael T, Pittner A, Rethmeier M. Microcrack formation during gas metal arc welding of high-strength fine-grained structural steel. Acta Metallurgica Sinica. English Letters. 2014;27(1):140-148. http://dx.doi.org/10.1007/s40195-013-0011-5.

[13] Stol I, Williams KL, Gaydos DW. Back to basics: using a buried gas metal arc for seam welds. Welding Journal. 2006;85(4):28-36.

[14] Chen J, Schwenk C, Wu CS, Rethmeier M. Predicting the influence of groove angle on heat transfer and fluid flow for new gas metal arc welding processes. International Journal of Heat and Mass Transfer. 2011;55:102-111. http://dx.doi.org/10.1016/j.ijheatmasstransfer.2011.08.046.

[15] Sproesser G, Chang Y-J, Pittner A, Finkbeiner M, Rethmeier M. Life Cycle Assessment of welding technologies for thick metal plate welds. Journal of Cleaner Production. 2015;108:46-53. http://dx.doi.org/10.1016/j.jclepro.2015.06.121.

[16] Yuan Y, Yamazaki K, Suzuki R. Relationship between penetration and porosity in horizontal fillet welding by a new process "hybrid tandem MAG welding process". Welding in the World. 2016;60(3):515-524. http://dx.doi.org/10.1007/s40194-016-0314-z.

[17] Pan Q, Mizutani M, Kawahito Y, Katayama S. Laser-arc hybrid welding of thick high tensile strength steel plates. In: Proceedings of the ICALEO® 2015: 34th International Congress on Laser Materials Processing, Laser Microprocessing and Nanomanufacturing; 2015; Atlanta, GA, USA. Vol. 495. Orlando, FL: Laser Institute of America; 2015. http://dx.doi.org/10.2351/1.5063199.

[18] Weman K. Welding processes handbook. 2nd ed. Cambridge: Woodhead; 2012. 270 p.

[19] Kou S. Welding metallurgy. 2nd ed. New Jersey: Welding Research Council; 2003. 461 p.

[20] Lancaster JF. The physics of welding. 2nd ed. Oxford: Pergamon; 1984. 340 p.

[21] Suban M, Tušek J. Methods for the determination of arc stability. Journal of Materials Processing Technology. 2003;143-144(1):430-437. http://dx.doi.org/10.1016/S0924-0136(03)00416-3.

[22] Díaz V, Acevedo F, Cunha T. Uma contribuição na determinação das variáveis da corrente contínua pulsada para o arame tubular E71T-1M. Soldagem e Inspeção. 2018;23(3):340-349. http://dx.doi.org/10.1590/0104-9224/si2303.04.

[23] Uribe A, Bracarense AQ, Pessoa ECP, Santos VR. Influência da polaridade sobre a estabilidade do processo de soldagem subaquática molhada com eletrodo revestido. Soldagem e Inspeção. 2017;22(4):429-441. http://dx.doi.org/10.1590/0104-9224/si2204.13.

[24] Scotti A, Ponomarev V. Soldagem MIG/MAG: melhor entendimento, melhor desempenho. São Paulo: Artliber; 2008. 284 p.

[25] Nogueira RMU, Bohórquez CEN, Zanella IG. Comparação da estabilidade do arco e da variabilidade da geometria de soldas obtidas pelos processos MIG/MAG e arame tubular. Soldagem e Inspeção. 2015;20(2):191-204. http://dx.doi.org/10.1590/0104-9224/SI2002.07.

[26] Warinsiriruk E, Poopat B. Investigation of metal transfer of ER70S-6 filler metal in MAG-M welding by acoustic signal detection. In: The Fourth Trailand Materials Science and Technologu Conference; 2006; Bangkok, Thailand. Thailand: National Metal and Materials Technology Center; 2006.

[27] Wahba M, Mizutani M, Katayama S. Hybrid welding with fiber laser and CO_2 gas shielded arc. Journal of Materials Processing Technology. 2015;221:146-153. http://dx.doi.org/10.1016/j.jmatprotec.2015.02.004.

[28] Katayama S. Handbook of laser welding technologies. 1st ed. Cambridge: Woodhead Publishing; 2013.

[29] Soderstrom E, Mendez P. Humping mechanisms present in high speed welding. Science and Technology of Welding and Joining. 2006;11(5):572-579. http://dx.doi.org/10.1179/174329306X120787.

[30] Gratzke U, Kapadia PD, Dowden J, Kroos J, Simon G. Theoretical approach to the humping phenomenon in welding processes. Journal of Physics. D, Applied Physics. 1992;25(11):1640-1647. http://dx.doi.org/10.1088/0022-3727/25/11/012.

[31] Chen J, Wu CS. Numerical simulation of humping phenomenon in high speed gas metal arc welding. Frontiers of Materials Science. 2011;5(2):90-97. http://dx.doi.org/10.1007/s11706-011-0123-7.

[32] Wei PS. Thermal science of weld bead defects: a review. Journal of Heat Transfer. 2011;133(3):031005. http://dx.doi.org/10.1115/1.4002445.